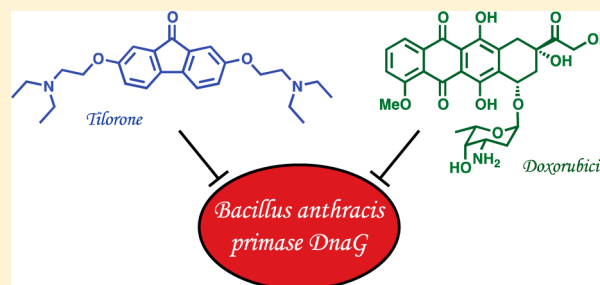


Discovery of Inhibitors of *Bacillus anthracis* Primase DnaGTapan Biswas,<sup>\*,†</sup> Keith D. Green,<sup>‡</sup> Sylvie Garneau-Tsodikova,<sup>‡</sup> and Oleg V. Tsodikov<sup>\*,‡</sup><sup>†</sup>Department of Medicinal Chemistry, College of Pharmacy, University of Michigan, Ann Arbor, Michigan 48109, United States<sup>‡</sup>Department of Pharmaceutical Sciences, University of Kentucky, Lexington, Kentucky 40536, United States

**ABSTRACT:** Primase DnaG is an essential bacterial enzyme that synthesizes short ribonucleotide primers required for chromosomal DNA replication. Inhibitors of DnaG can serve as leads for development of new antibacterials and biochemical probes. We recently developed a nonradioactive *in vitro* primase–pyrophosphatase assay to identify and analyze DnaG inhibitors. Application of this assay to DnaG from *Bacillus anthracis* (*Ba* DnaG), a dangerous pathogen, yielded several inhibitors, which include agents with DNA intercalating properties (doxorubicin and tilorone) as well as those that do not intercalate into DNA (suramin). A polyanionic agent and inhibitor of eukaryotic primases, suramin, identified by this assay as a low-micromolar *Ba* DnaG inhibitor, was recently shown to be also a low-micromolar inhibitor of *Mycobacterium tuberculosis* DnaG (*Mtb* DnaG). In contrast, another low-micromolar *Ba* DnaG inhibitor, tilorone, is much more potent against *Ba* DnaG than against *Mtb* DnaG, despite homology between these enzymes, suggesting that DnaG can be targeted selectively.



DNA polymerases cannot initiate DNA synthesis *de novo*, i.e., by using single-stranded DNA as a template; they require short oligoribonucleotide primers synthesized by a poorly processive polymerase called primase. This function of primase in chromosomal DNA replication is conserved in all organisms. In bacteria, only the DnaG protein functions as a primase in replication of chromosomal DNA, and therefore, DnaG is essential for cell division. This essentiality has been demonstrated directly in several diverse bacteria, such as *Escherichia coli*,<sup>1,2</sup> *Bacillus subtilis*,<sup>3</sup> and *Mycobacterium smegmatis*,<sup>4</sup> through the use of temperature-sensitive DnaG mutants. Because of the essentiality of DnaG and its divergence from the eukaryotic primase, DnaG is an attractive target for antibacterial drug discovery.<sup>5,6</sup> In addition, the level of conservation of DnaG among bacteria that are phylogenetically distant is only modest (e.g., 30% identical sequences of *Bacillus* and *Mycobacterium* primases), allowing the possibility that a narrow-spectrum antibacterial DnaG inhibitor may be discovered. Discovery of inhibitors of DnaG that could serve as leads for development of antibacterials or biochemical probes is in its infancy. We recently developed a nonradioactive *in vitro* primase–pyrophosphatase assay, in which the primer synthesis by DnaG is coupled to cleavage of the liberated pyrophosphate (PP<sub>i</sub>) to inorganic phosphate (P<sub>i</sub>) by an inorganic pyrophosphatase (PPiase). The P<sub>i</sub> product is then detected through its reaction with a malachite green reagent.<sup>7</sup> We adapted this assay for high-throughput screening (HTS) of large libraries of chemicals and applied it to successfully identify several inhibitors of *Mycobacterium tuberculosis* DnaG (*Mtb* DnaG) from a pilot library of drug and druglike compounds.<sup>7</sup> In this study, we performed a similar pilot HTS to discover inhibitors of DnaG from the *Bacillus anthracis* 34F2 Sterne strain (*Ba*

DnaG), a dangerous pathogen. The assay was also used to analyze inhibition properties of selected compounds.

## ■ MATERIALS AND METHODS

**Cloning and Purification of *Ba* DnaG, *Mtb* DnaG, and *Mtb* PPiase.** The primase gene *dnaG* (locus tag BAS4195) was amplified by PCR from genomic DNA of the *B. anthracis* 34F2 Sterne strain (*Ba*) by using primers (5'-AGTTAGCACATA-TGGGGAACAGAATTCCTGAAG-3') and (5'-CTCCGCT-CGAGCTATTTTCTCGCTTTTGATTTTG-3') and cloned between the *Nde*I and *Xho*I sites of a modified pET19b vector,<sup>8</sup> encoding an N-terminal decahistidine tag separated from the recombinant protein by a PreScission protease (GE Healthcare, Piscataway, NJ) cleavage site. The *Ba* DnaG protein was expressed and purified according to a previously published protocol for *Mtb* DnaG.<sup>7</sup> *Mtb* DnaG and *Mtb* PPiase were purified as previously described.<sup>7</sup>

**Primer Synthesis Assay.** Primer synthesis reactions used to obtain radioactively labeled primers were performed as follows. The reaction mixtures contained 1 μM *Ba* DnaG, 1 μM single-stranded DNA 32-mer 5'-GAAGCACCAGACGTTTACATACATTCACAGA-3', and NTPs (100 μM each) in buffer containing 20 mM CAPS (pH 8.8), 150 mM potassium glutamate, 2 mM MnCl<sub>2</sub>, 1 mM DTT, and 110 nM [α-<sup>32</sup>P]GTP. Reaction mixtures were incubated at 22 °C for 30 min. The products were phenol extracted and separated by 12% urea–polyacrylamide gel electrophoresis. The primer

Received: August 16, 2013

Revised: September 3, 2013

Published: September 4, 2013

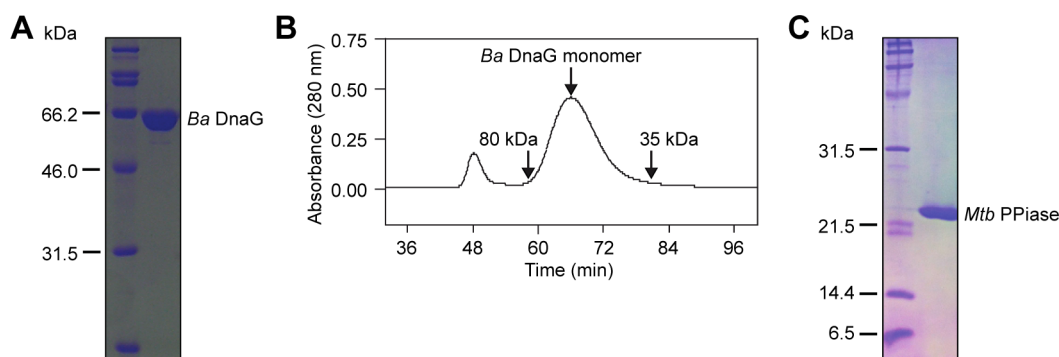


**Figure 1.** Coomassie blue-stained sodium dodecyl sulfate–polyacrylamide gel electrophoresis gels of pure (A) *Ba* DnaG and (C) *Mtb* PPiase. (B) S200 size-exclusion chromatogram of the purified *Ba* DnaG monomer.

products were visualized with a Typhoon phosphorimager system (GE Healthcare).

**High-Throughput Screening (HTS) Assay.** The HTS assay was performed as previously described in detail,<sup>7</sup> and the sequence of the DNA template is given in the previous section, except for changes in the final concentrations of *Ba* DnaG and the library compounds (4 and 30  $\mu$ M, respectively). EDTA at the final concentration of 30 mM was added to the last two columns of wells of each 384-well plate as a positive inhibition control. We used a library containing 2556 compounds (Spectrum Chemicals, New Brunswick, NJ). The library included 2000 compounds approved by the Food and Drug Administration, kinase inhibitors, and other compounds that have been used in human therapy.

The  $Z'$  score was calculated by using the following equation:<sup>9</sup>

$$Z' = 1 - 3 \frac{SD(\text{pos}) + SD(\text{neg})}{|Av(\text{pos}) - Av(\text{neg})|} \quad (1)$$

where  $Av(\text{pos})$  and  $SD(\text{pos})$  are the signal (absorbance) and its standard deviation for the positive controls, respectively (EDTA-containing reaction mixtures), and  $Av(\text{neg})$  and  $SD(\text{neg})$  are the respective values for negative controls (inert compounds).

**Coupled Colorimetric Primase–Pyrophosphatase Assay Used for Quantitative Inhibition Analysis.** The assay used in the quantitative analysis of inhibition was performed in 96-well clear polystyrene plates (Fisher Scientific, Pittsburgh, PA) as previously reported<sup>7</sup> and with the DNA template defined above and 4  $\mu$ M *Ba* DnaG. The reaction mixture contained DNA (1.25  $\mu$ M or as specified), NTP (110  $\mu$ M or as specified), 50 mM NaCl, 150 mM potassium glutamate, buffer [20 mM CAPS (pH 8.8) or as specified], and divalent metals (2 mM  $Mn^{2+}$  and 1 mM  $Mg^{2+}$ ). *Mtb* PPiase was used at a final concentration of 50 nM. For measurements of the activity of *Mtb* PPiase, the same reaction conditions were used except sodium pyrophosphate (100  $\mu$ M) was used in the reaction mixture instead of *Ba* DnaG, DNA, and NTP.

Dose–response assays were performed as previously described.<sup>7</sup> The dose–response curves were analyzed by nonlinear regression fitting to the following equation with  $IC_{50}$  as a fitting parameter using SigmaPlot 9.0 (SysStat Software, San Jose, CA):

$$f = \frac{1}{1 + \left(\frac{[I]}{IC_{50}}\right)^n} \quad (2)$$

where  $f$  is the fraction of activity,  $[I]$  is the inhibitor concentration, and  $n$  is the Hill coefficient.

**Mode of Inhibition Assays and Analysis.** The assays were performed and quantified as described previously,<sup>10</sup> except that *Ba* DnaG (4  $\mu$ M) was used. We ran two sets of reactions: (1) at a constant DNA concentration of 1.25  $\mu$ M at different concentrations of NTP (31.25, 62.5, 125, and 250  $\mu$ M) and (2) at a constant NTP concentration of 110  $\mu$ M at different concentrations of DNA (0.19, 0.38, 0.75, and 1.5  $\mu$ M). In each case, several concentrations (0, 1.25, 2.5, 5, 10, 20, and 40  $\mu$ M) of tilorone were used. The data were analyzed as previously described,<sup>7</sup> by assuming an ordered sequential rapid equilibrium mechanism of RNA synthesis by DnaG, in which DNA binds free DnaG first, followed by the first NTP and subsequent cycles of binding and incorporation of an average of  $m$  nucleotides (releasing  $m$   $PP_i$  molecules), and dissociation of DnaG from DNA. For a DnaG inhibitor that binds DNA (instead of DnaG) with equilibrium binding constant  $K_i$  to a good approximation in excess of the inhibitor (I) one obtains the concentration of DnaG-accessible DNA sites  $[S]$  in relationship to the total concentration of sites  $[S]_T$ :

$$[S] = [S]_T \left( \frac{K_i}{K_i + [I]} \right) \quad (3)$$

Then in the classical Michaelis–Menten equation, substrate concentration  $[S]$  needs to be substituted according to eq 3, which results in the equation equivalent to that describing competitive inhibition, where the inhibitor binds the enzyme.

***B. anthracis* Culture Assays and MIC Measurements.** To test the antibacterial activity of doxorubicin and tilorone, various amounts (2–20  $\mu$ g) of compound were spotted on sterile filter disks (5 mm in diameter, cut of Whatman #52 filter paper) and allowed to air-dry for 30 min. The disks were then placed on plates covered with soft brain heart infusion (BHI) agar [0.75% (w/v)] containing the *B. anthracis* 34F2 Sterne strain (100  $\mu$ L of a turbid culture per 25 mL of soft BHI agar). The bacteria were allowed to grow overnight (~16 h) at 37  $^{\circ}$ C and visualized. Doxorubicin showed a zone of inhibition at 6  $\mu$ g, while tilorone showed no zone of inhibition up to 20  $\mu$ g.

MIC values for doxorubicin were determined for the *B. anthracis* 34F2 Sterne strain by the double-dilution method starting at 120  $\mu$ g/mL. All experiments were performed in triplicate and values confirmed by the addition of 3-(4,5-dimethylthiazol-2-yl)-2,5-diphenyltetrazolium bromide (MTT; 50  $\mu$ L of a 1 mg/mL solution in water). The MIC reactions that resulted in no growth were then used to determine if the drug was bactericidal or bacteriostatic by plating 20  $\mu$ L of the MIC

reaction mixture onto a fresh BHI plate. The plates were incubated overnight (~16 h) at 37 °C, and in the case of doxorubicin, growth was observed at all concentrations, indicative of bacteriostatic activity.

## RESULTS AND DISCUSSION

**High-Throughput Screening (HTS) To Identify Inhibitors of *Ba* DnaG.** *Ba* DnaG was cloned, overexpressed in *E. coli*, and purified to homogeneity (Figure 1) following a protocol similar to the one that we recently developed for *Mtb* DnaG.<sup>10</sup> To identify inhibitors of *Ba* DnaG, we used our recently reported novel colorimetric primase–PPiase assay in HTS of a library of 2556 diverse compounds, most of which have been in clinical use in humans. We used *Mtb* PPiase as the coupled enzyme, because of its proven efficiency.<sup>7,11,12</sup> The HTS assay was robust ( $Z' > 0.6$ ) and yielded nine compounds that displayed inhibition larger than three standard deviations ( $3\sigma$ ) of the signal from inert compounds, when  $\sigma$  was calculated over all compounds of the assay (Figure 2). When

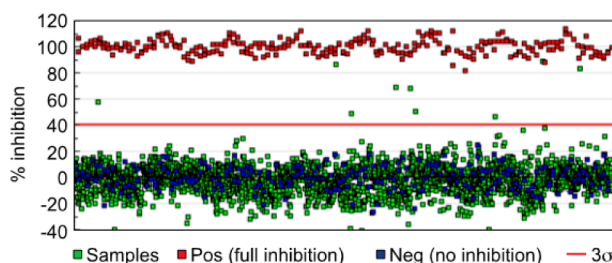


**Figure 2.** Scatter plot of the HTS of *Ba* DnaG and *Mtb* PPiase. The red line denotes the three-standard deviation ( $3\sigma$ ) inhibition level. The red squares denote 100% inhibition by 30 mM EDTA.

the values of  $\sigma$  were calculated for each plate, 21 compounds displayed the level of inhibition over  $3\sigma$ . These compounds included anticancer anthracyclines doxorubicin and epirubicin, interferon inducer tilorone, fluoroquinolone antibiotics levofloxacin, enrofloxacin, and rifloxacin, and antiparasitic agent suramin. These compounds did not display inhibitory activity against *Mtb* PPiase; therefore, we investigated the effect of the representatives of each structural class on the activity of *Ba* DnaG.

**Inhibition of *Ba* DnaG and *Mtb* DnaG by Doxorubicin and Tilorone.** We tested inhibition of the priming activity of *Ba* DnaG by doxorubicin and tilorone directly, by monitoring formation of radioactively labeled RNA primers under the conditions of the colorimetric assay. Both compounds inhibited *Ba* DnaG in the low-micromolar range (Figure 3). Doxorubicin was previously identified as a low-micromolar inhibitor of *Mtb* DnaG by a similar HTS of the same compound library,<sup>7</sup> whereas tilorone was not. We measured the dose response of inhibition of *Ba* DnaG and *Mtb* DnaG by doxorubicin and tilorone by the colorimetric assay (Figure 4). Indeed, tilorone displayed approximately 10-fold better inhibition of *Ba* DnaG [ $IC_{50} = 7.1 \pm 0.7 \mu M$  ( $n = 1$ )] than of *Mtb* DnaG [ $IC_{50} = 69 \pm 5 \mu M$  ( $n = 1$ )], whereas the potency of doxorubicin against *Ba* DnaG was only ~2-fold higher than that against *Mtb* DnaG [ $IC_{50} = 4.4 \pm 0.3 \mu M$  ( $n = 1.8 \pm 0.2$ ) and  $IC_{50} = 9.3 \pm 0.2 \mu M$  ( $n = 2.3 \pm 0.1$ ), respectively]. Therefore, tilorone is a species-selective inhibitor of DnaG, demonstrating a potential for discovery of narrow-spectrum agents against this target. Doxorubicin is an antibiotic natural product that has been

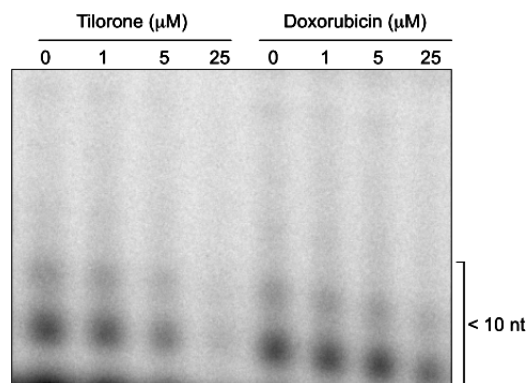


**Figure 3.** Inhibition of primer synthesis by tilorone and doxorubicin. A denaturing urea–polyacrylamide gel electrophoresis gel demonstrates synthesis of short (<10 nucleotides) radioactively labeled primers by *Ba* DnaG as a function of tilorone and doxorubicin concentration.

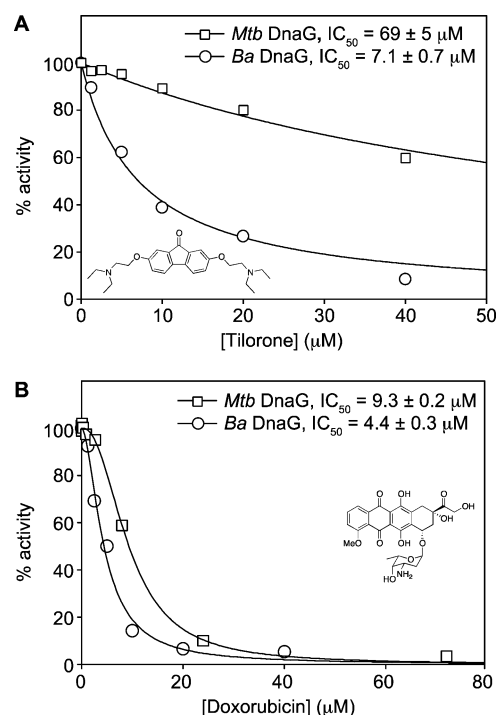


**Figure 4.** Primase–PPiase dose–response assays with (A) tilorone and (B) doxorubicin with *Ba* DnaG (○) and *Mtb* DnaG (□). The doxorubicin inhibition data for *Mtb* DnaG were previously reported.<sup>7</sup>

used in the clinic as an anticancer agent, because of its potent inhibition of topoisomerase II in eukaryotic cells.<sup>13</sup> In contrast, the mechanism of action of doxorubicin against bacteria has remained elusive. In fact, doxorubicin is a poor (~100  $\mu M$ ) inhibitor of DNA gyrase,<sup>14</sup> an essential enzyme homologous to topoisomerase II in bacteria. Intriguingly, even though DnaG is negligibly homologous in sequence with topoisomerase II or gyrase, its catalytic domains share the same TOPRIM fold, which is implicated in nucleotide binding and catalysis. This and the previous study by our group,<sup>10</sup> therefore, indicate that DnaG is likely a doxorubicin target in bacteria.

**Mode of Inhibition of Activity of *Ba* DnaG by Tilorone.** To gain insight into the mechanism of inhibition of *Ba* DnaG by tilorone, we performed a series of steady-state measurements of the release of PP<sub>i</sub> at different concentrations of tilorone, NTP, and DNA template (Figure 5). The data



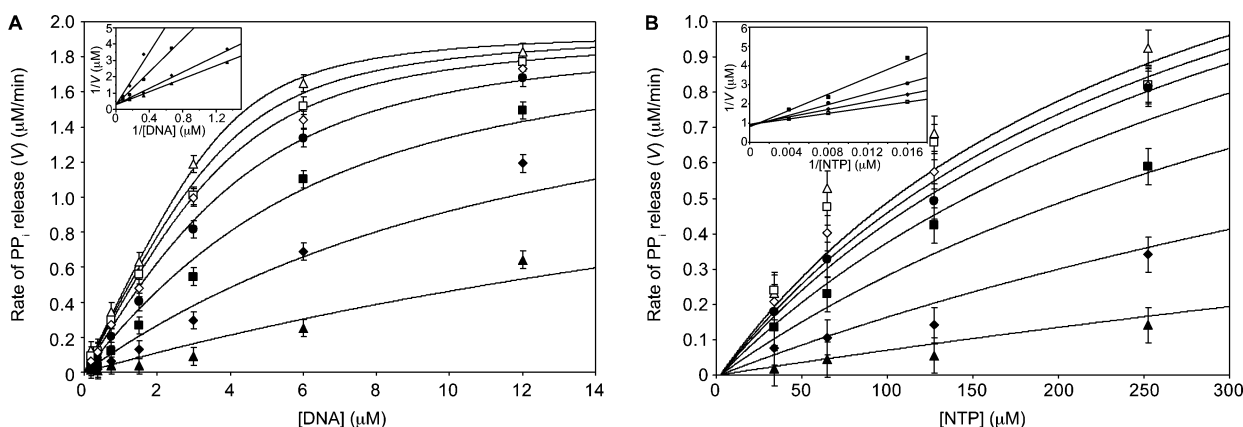


**Figure 5.** Dependence of the rate of the steady-state  $\text{PP}_i$  release as a result of primer synthesis by *Ba* DnaG on concentrations of tilorone, DNA, and NTP. The rate of  $\text{PP}_i$  release was measured as a function of (A) DNA concentration or (B) NTP concentration for the following concentrations of tilorone: 0 ( $\Delta$ ), 1.25 ( $\square$ ), 2.5 ( $\diamond$ ), 5 ( $\bullet$ ), 10 ( $\blacksquare$ ), 20 ( $\blacklozenge$ ), and 40  $\mu\text{M}$  ( $\blacktriangle$ ). The curves correspond to the fit of all the data to the kinetic mechanism described in the text. The insets show subsets of these data as Lineweaver–Burk plots to demonstrate the apparent competitive inhibition mode of tilorone with DNA and NTP.

demonstrate that tilorone is competitive with respect to both DNA and NTP (Figure 5, inset). When interpreted in terms of a simple slow initiation–rapid elongation primer synthesis mechanism, which was previously applied to *Mtb* DnaG, the nonlinear regression analysis of these inhibition data (Figure 5) indicate a binding stoichiometry of one to two molecules of tilorone per *Ba* DnaG. If their affinities ( $K_i$ ) are the same, we obtain a  $K_i$  of  $2.3 \pm 0.6 \mu\text{M}$ . The analysis also yielded the equilibrium constants for an incoming NTP binding to *Ba* DnaG ( $K_{\text{NTP}} = 140 \pm 20 \mu\text{M}$ ), the apparent catalytic rate constant for NTP incorporation ( $k_{\text{cat}} = 1.06 \pm 0.06 \text{ min}^{-1}$ ), and an upper bound on the template DNA binding constant ( $K_{\text{DNA}} < 300 \text{ nM}$ ). A more complex model, in which one molecule of tilorone binds *Ba* DnaG with a higher affinity ( $\sim 1 \mu\text{M}$ ) than the other ( $\sim 10 \mu\text{M}$ ), fits the data equally well. However, the large number of fitting parameters in this and other more complex models does not allow us to resolve whether multiple molecules bind with the same affinity or different affinities. As tilorone is a DNA intercalator that binds DNA with a  $K_d$  in the low-micromolar range (per base),<sup>15,16</sup> on the basis of these data alone, we cannot exclude a model in which one or more tilorone molecules bind DNA, thereby blocking primer synthesis by *Ba* DnaG or forming a nonproductive ternary complex. Within the experimental uncertainty, such a mode of inhibition (also competitive) cannot be distinguished by the experiments described above (see Materials and Methods), and the  $K_i$  values obtained above are interpreted as the equilibrium constants for binding of tilorone to DNA. Within the framework of the model of tilorone inhibition by DNA binding rather than enzyme binding, the selectivity of tilorone against *Ba* DnaG over *Mtb* DnaG means that *Mtb* DnaG is able to actively displace tilorone from DNA more readily than *Ba* DnaG. For doxorubicin, this inhibition model means that neither DnaG can readily displace doxorubicin bound to DNA.

#### Inhibition of *Ba* DnaG by Suramin and Levofloxacin.

Another HTS hit, the antiprotozoan drug suramin, was recently identified and characterized as a low-micromolar inhibitor of *Mtb* DnaG. Suramin strongly inhibits eukaryotic primase by competitively binding to the respective binding sites on this enzyme and displays inhibitory activity against other eukaryotic nucleic acid and nucleotide binding enzymes.<sup>17</sup> A competitive mode of inhibition of suramin with DNA and NTP was also

demonstrated for *Mtb* DnaG.<sup>10</sup> In a dose–response assay, suramin exhibited strong inhibitory activity against *Ba* DnaG, with an  $\text{IC}_{50}$  of  $8.2 \pm 1.3 \mu\text{M}$  (Figure 6). Another HTS hit,

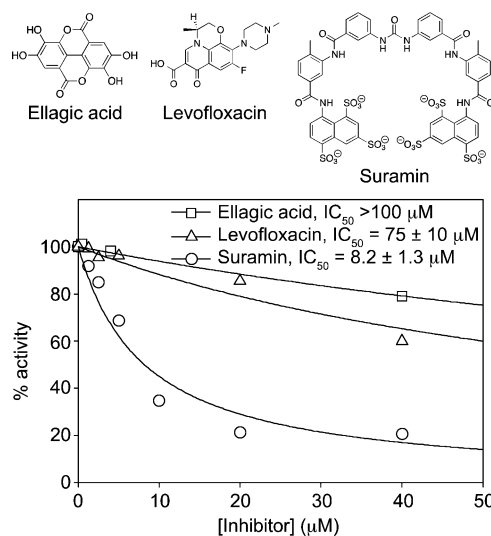


**Figure 6.** Primase– $\text{PP}_i$ ase dose–response assays with ellagic acid ( $\square$ ), levofloxacin ( $\Delta$ ), and suramin ( $\circ$ ) with *Ba* DnaG.

levofloxacin, is a clinically used fluoroquinolone antibiotic that acts by trapping a DNA gyrase–DNA complex in a state on the mechanism pathway in which the DNA contains a double-strand break. The generation of double-strand breaks ultimately leads to the bactericidal effect of fluoroquinolones. The dose–response assay for levofloxacin with *Ba* DnaG indicates the weak inhibitory activity of this compound, with an  $\text{IC}_{50}$  of  $75 \pm 10 \mu\text{M}$  (Figure 6). Inhibition of DnaG by quinolones has not been previously reported and, consistent with the observed weak levofloxacin inhibition of DnaG *in vitro*, is likely insignificant *in vivo*, at least at sub-micromolar to low-micromolar concentrations of the drug. Indeed, point mutations in gyrase genes can cause loss of quinolone binding and high levels of quinolone resistance, increasing the MIC to  $\sim 100 \mu\text{M}$ . Finally, we tested ellagic acid, a  $20 \mu\text{M}$  inhibitor of *Mtb* DnaG,<sup>10</sup> which to our surprise was not an HTS hit with *Ba* DnaG, despite a higher concentration of the compound used in

this screening. Indeed, ellagic acid displayed extremely weak inhibitory activity against *Ba* DnaG ( $IC_{50} > 100 \mu M$ ) (Figure 6), further supporting the notion that DnaG inhibitors can be species-specific.

**Activity of HTS Hits against *Ba* Cells in an *in Vitro* Culture Assay.** Only a subset of DnaG inhibitors that were discovered by HTS using *in vitro* enzymatic assays are predicted to be active because of the inability of many compounds to penetrate the bacterial envelope and reach their cytoplasmic target. Doxorubicin, which is able to penetrate readily into the cytoplasm of both Gram-positive and Gram-negative bacteria, exhibited a bacteriostatic inhibitory activity toward an *in vitro* culture of the *Ba* 34F2 Sterne strain. A measurement of the MIC yielded a value of  $6.6 \mu M$ , consistent with the  $IC_{50}$  value measured *in vitro*. Even though DnaG may not be the only molecular target of doxorubicin in *Ba*, the bacteriostatic mode of killing by doxorubicin is consistent with inhibition of DNA replication. Tilorone and suramin were inactive against the bacilli, likely because they could not penetrate the bacterial cell envelope. Levofloxacin is a well-documented potent inhibitor of *Ba* both in *in vitro* cultures<sup>18</sup> and in the animal models of inhalation anthrax because of its activity against gyrase.<sup>19</sup>

## CONCLUSIONS

In summary, we have conducted a primase–PPiase HTS assay, which yielded tilorone, doxorubicin, and suramin as potent inhibitors of *Ba* DnaG. Doxorubicin is likely a broad-spectrum inhibitor of DnaG *in vivo*, and ongoing studies are aimed at clarifying its mode of action in the bacterial cell. On the other hand, the inhibitory potency of tilorone against *Ba* DnaG is stronger than that against *Mtb* DnaG. Similarly, ellagic acid is a weak but selective inhibitor of *Mtb* DnaG over *Ba* DnaG. Even though neither tilorone nor ellagic acid is active against bacterial cultures, each serves as a proof of principle for identifying and developing selective narrow-spectrum DnaG inhibitors as chemical probes and leads for development of new antibiotics in future studies. Our HTS assay, now used successfully against two different primases, is a useful method for these studies.

## AUTHOR INFORMATION

### Corresponding Authors

\*Email: oleg.tsodikov@uky.edu. Phone: (859) 218-1687. Fax: (859) 257-7585.

\*E-mail: t.biswas@yahoo.com.

### Author Contributions

T.B. and K.D.G. performed the experiments. T.B., O.V.T., and K.D.G. analyzed the data. S.G.-T. and O.V.T. wrote the manuscript. All authors performed editing and have given approval to the final version of the manuscript.

### Funding

This work was supported by start-up funds from University of Michigan College of Pharmacy and from the University of Kentucky (to O.V.T. and S.G.-T.).

### Notes

The authors declare no competing financial interests.

## ACKNOWLEDGMENTS

We thank Tom McQuade and Dr. Martha Larsen at the Center for Chemical Genomics at the University of Michigan for their assistance with the HTS. We thank Dr. Luiz Pedro de Carvalho for a generous gift of the *Mtb* PPiase expression vector.

## ABBREVIATIONS

*Ba*, *B. anthracis*; CAPS, *N*-cyclohexyl-3-aminopropanesulfonic acid; DTT, dithiothreitol; EDTA, ethylenediaminetetraacetic acid; HTS, high-throughput screening; MIC, minimal inhibitory concentration; *Mtb*, *M. tuberculosis*; NTP, nucleoside triphosphate; PCR, polymerase chain reaction.

## REFERENCES

- (1) Gefter, M. L., Hirota, Y., Kornberg, T., Wechsler, J. A., and Barnoux, C. (1971) Analysis of DNA polymerases II and 3 in mutants of *Escherichia coli* thermosensitive for DNA synthesis. *Proc. Natl. Acad. Sci. U.S.A.* 68, 3150–3153.
- (2) van der Ende, A., Baker, T. A., Ogawa, T., and Kornberg, A. (1985) Initiation of enzymatic replication at the origin of the *Escherichia coli* chromosome: Primase as the sole priming enzyme. *Proc. Natl. Acad. Sci. U.S.A.* 82, 3954–3958.
- (3) Karamata, D., and Gross, J. D. (1970) Isolation and genetic analysis of temperature-sensitive mutants of *B. subtilis* defective in DNA synthesis. *Mol. Gen. Genet.* 108, 277–287.
- (4) Klann, A. G., Belanger, A. E., Abanes-De Mello, A., Lee, J. Y., and Hatfull, G. F. (1998) Characterization of the *dnaG* locus in *Mycobacterium smegmatis* reveals linkage of DNA replication and cell division. *J. Bacteriol.* 180, 65–72.
- (5) Kuchta, R. D., and Stengel, G. (2010) Mechanism and evolution of DNA primases. *Biochim. Biophys. Acta* 1804, 1180–1189.
- (6) Sanyal, G., and Doig, P. (2012) Bacterial DNA replication enzymes as targets for antibacterial drug discovery. *Expert Opin. Drug Discovery* 7, 327–339.
- (7) Biswas, T., Resto-Roldan, E., Sawyer, S. K., Artsimovitch, I., and Tsodikov, O. V. (2013) A novel non-radioactive primase-pyrophosphatase activity assay and its application to the discovery of inhibitors of *Mycobacterium tuberculosis* primase DnaG. *Nucleic Acids Res.* 41, e56.
- (8) Biswas, T., and Tsodikov, O. V. (2008) Hexameric ring structure of the N-terminal domain of *Mycobacterium tuberculosis* DnaB helicase. *FEBS J.* 275, 3064–3071.
- (9) Zhang, J. H., Chung, T. D., and Oldenburg, K. R. (1999) A simple statistical parameter for use in evaluation and validation of high throughput screening assays. *J. Biomol. Screening* 4, 67–73.
- (10) Biswas, T., Resto-Roldan, E., Sawyer, S. K., Artsimovitch, I., and Tsodikov, O. V. (2013) A novel non-radioactive primase-pyrophosphatase activity assay and its application to the discovery of inhibitors of *Mycobacterium tuberculosis* primase DnaG. *Nucleic Acids Res.* 41, e56.
- (11) Tammenkoski, M., Benini, S., Magretova, N. N., Baykov, A. A., and Lahti, R. (2005) An unusual, His-dependent family I pyrophosphatase from *Mycobacterium tuberculosis*. *J. Biol. Chem.* 280, 41819–41826.
- (12) Rodina, E. V., Vainonen, L. P., Vorobyeva, N. N., Kurilova, S. A., Sitnik, T. S., and Nazarova, T. I. (2008) Metal cofactors play a dual role in *Mycobacterium tuberculosis* inorganic pyrophosphatase. *Biochemistry (Moscow)* 73, 897–905.
- (13) Patel, S., Sprung, A. U., Keller, B. A., Heaton, V. J., and Fisher, L. M. (1997) Identification of yeast DNA topoisomerase II mutants resistant to the antitumor drug doxorubicin: Implications for the mechanisms of doxorubicin action and cytotoxicity. *Mol. Pharmacol.* 52, 658–666.
- (14) Glaser, B. T., Malerich, J. P., Duellman, S. J., Fong, J., Hutson, C., Fine, R. M., Keblansky, B., Tang, M. J., and Madrid, P. B. (2011) A high-throughput fluorescence polarization assay for inhibitors of gyrase B. *J. Biomol. Screening* 16, 230–238.
- (15) Chandra, P., Zunino, F., Gaur, V. P., Zaccara, A., Woltersdorf, M., Luoni, G., and Gotz, A. (1972) Mode of tilorone hydrochloride interaction to DNA and polydeoxyribonucleotides. *FEBS Lett.* 28, 5–9.
- (16) Chandra, P., Zunino, F., Zaccara, A., Wacker, A., and Gotz, A. (1972) Influence of tilorone hydrochloride on the secondary structure and template activity of DNA. *FEBS Lett.* 23, 145–148.
- (17) Ono, K., Nakane, H., and Fukushima, M. (1988) Differential inhibition of various deoxyribonucleic and ribonucleic-acid polymerases by suramin. *Eur. J. Biochem.* 172, 349–353.

(18) Bast, D. J., Athamna, A., Duncan, C. L., de Azavedo, J. C., Low, D. E., Rahav, G., Farrell, D., and Rubinstein, E. (2004) Type II topoisomerase mutations in *Bacillus anthracis* associated with high-level fluoroquinolone resistance. *J. Antimicrob. Chemother.* 54, 90–94.

(19) Peterson, J. W., Moen, S. T., Healy, D., Pawlik, J. E., Taormina, J., Hardcastle, J., Thomas, J. M., Lawrence, W. S., Ponce, C., Chatuev, B. M., Gnade, B. T., Foltz, S. M., Agar, S. L., Sha, J., Klimpel, G. R., Kirtley, M. L., Eaves-Pyles, T., and Chopra, A. K. (2010) Protection afforded by fluoroquinolones in animal models of respiratory infections with *Bacillus anthracis*, *Yersinia pestis*, and *Francisella tularensis*. *Open Microbiol. J.* 4, 34–46.